Article

Discovery Medicine 2025; 37(198): 1385–1398
https://doi.org/10.24976/Discov.Med.202537198.120

Mechanisms of Loxo-305 in Treating Rheumatoid Arthritis by Dual Inhibition of B Cell Activity and Osteoclast Differentiation

Xuena Wang[1], Lianjie Cheng[2], Aihua Liu[1,*]

[1]Department of Rheumatology, Shandong Provincial Third Hospital, Shandong University, 250031 Jinan, Shandong, China
[2]Department of Hand & Foot and Reconstructive Microsurgery, Shandong Provincial Hospital Affiliated to Shandong First Medical University, 250000 Jinan, Shandong, China
*Correspondence: lkt181022@126.com (Aihua Liu)
Published: 20 July 2025

Background: Rheumatoid arthritis (RA) is a chronic inflammatory autoimmune disease characterized by joint inflammation and damage. The aim of this study was to evaluate the therapeutic effects of Loxo-305, a novel treatment, on RA in a mouse model.

Methods: Through intravenous injection of collagen-Complete Freund's Adjuvant (CFA) emulsion (100 µL), Dilute Brown Non-Agouti 1 (DBA/1) mice were induced with RA. Two weeks after immunization, the severity of joint swelling was assessed. Mice in the low-dose and high-dose Loxo-305 groups were treated with 10 mg/kg/day and 20 mg/kg/day of Loxo-305, respectively, for 2 weeks, while animals in the control and model groups were administered saline. The mice were euthanized after the treatment period, and their peripheral blood, spleen, and joint tissues were collected for analysis. Histological analysis of joint tissues was performed using hematoxylin and eosin (HE) staining, and osteoclastogenesis was evaluated using tartrate-resistant acid phosphatase (TRAP) staining. The expression of Cluster of Differentiation 19 (CD19), Receptor Activator of Nuclear Factor Kappa-B Ligand (RANKL), and Cluster of Differentiation 11b (CD11b) in tissues was detected by means of immunohistochemistry (IHC). Spleen cells were isolated and stimulated with anti-immunoglobulin M (IgM) antibodies to induce B cell differentiation. Cell proliferation was assessed using 5-ethynyl-2′-deoxyuridine staining (EdU) staining, and B cell activation was analyzed by flow cytometry. Serum immunoglobulin and inflammatory cytokine levels were measured through enzyme-linked immunosorbent assay (ELISA), and quantitative real-time polymerase chain reaction (qRT-PCR) was used to quantify the expression of osteoclast-related genes in joint tissues.

Results: Loxo-305 effectively inhibited the progression of RA in mice, significantly reducing paw swelling, synovial hyperplasia, inflammatory cell infiltration, cartilage erosion, and bone destruction in a dose-dependent manner ($p < 0.05$). It attenuated osteoclast formation, inhibited B cell activation, and reduced plasma cell numbers and serum immunoglobulin G (IgG) levels ($p < 0.05$). Loxo-305 also decreased the expression of TRAP, Dendritic Cell-Specific Transmembrane Protein (DC-STAMP), Cathepsin K (CTSK), and RANKL while increasing Osteoprotegerin (OPG) levels in joint tissues ($p < 0.05$) and significantly suppressed joint inflammation by reducing interleukin (IL)-6, tumor necrosis factor alpha (TNF-α), IL-1β, and CD11b expression ($p < 0.05$).

Conclusions: Loxo-305 effectively inhibits the progression of RA by suppressing osteoclastogenesis, B cell and plasma cell activation, and reducing the expression of inflammatory cytokines and RANKL, demonstrating significant therapeutic potential. Loxo-305 effectively controls the progression of RA through a dual mechanism of "immune regulation and bone protection". Compared to existing Bruton's tyrosine kinase (BTK) inhibitors, it offers superior target specificity, safety, and breadth of action, highlighting its potential and promising clinical translational value in the treatment of RA.

Keywords: Rheumatoid arthritis; Loxo-305; B cell; osteoclast

Introduction

Rheumatoid arthritis (RA) is a chronic, systemic autoimmune disease primarily characterized by synovial inflammation, joint destruction, and multi-organ damage [1, 2]. The etiology of RA is complex, involving various genetic, environmental factors, and abnormal activation of the immune system [3,4]. The main pathological features of the disease include proliferation of synovial cells, infiltration of immune cells, pannus formation, and destruction of cartilage and bone [5,6]. These pathological processes not only lead to joint pain, swelling, and dysfunction, but also, in severe cases, can result in joint deformities and permanent disability [7].

Although significant progress has been made in RA treatment in recent years, especially with the use of bio-

logics (such as tumor necrosis factor alpha [TNF-α] inhibitors and interleukin [IL]-6 receptor blockers) and small molecule drugs (such as Janus kinase [JAK] inhibitors), which have greatly improved the prognosis for RA patients, complete disease remission is still not achievable in a considerable number of patients [8,9]. These patients may develop resistance to existing medications or experience serious side effects associated with long-term drug use [10]. Therefore, the development of new drugs with distinct mechanisms of action, significant efficacy, and fewer side effects remains a crucial research direction in the field of RA treatment.

In the pathological process of RA, B cells and osteoclasts are considered key effector cells [11,12]. B cells play a central role in the pathogenesis of RA by producing autoantibodies, activating other immune cells, amplifying the inflammatory response, and contributing to osteoclastogenesis [13,14]. Osteoclasts, on the other hand, are the primary effector cells responsible for bone destruction in RA. Their excessive activity leads to increased bone resorption, erosion of trabecular bone structure, and ultimately loss of joint function [15,16]. Therefore, therapies targeting B cells and osteoclasts hold significant potential in the treatment of RA.

Bruton's tyrosine kinase (BTK) is a key enzyme in the B cell receptor (BCR) signaling pathway, directly involved in the activation, proliferation, and differentiation of B cells [17]. BTK not only plays an essential role in B cells but also regulates the function of other immune cells such as macrophages, dendritic cells, and osteoclasts, making it an important therapeutic target in RA and other autoimmune diseases [18]. In recent years, BTK inhibitors have shown promising therapeutic potential in animal models of RA and systemic lupus erythematosus, significantly reducing joint inflammation and bone destruction by inhibiting the activity of B cells and osteoclasts [19].

Loxo-305 is a novel BTK inhibitor with highly selective and potent BTK inhibition [20]. Compared to other BTK inhibitors, Loxo-305 can achieve complete inhibition of BTK without affecting other tyrosine kinases, thereby minimizing side effects [21]. While the efficacy of Loxo-305 has been preliminarily validated in certain hematological malignancies, its mechanisms of action and therapeutic efficacy in RA animal models have yet to be fully explored.

To this end, this study systematically evaluated the effects of Loxo-305 in the treatment of RA using a collagen-induced arthritis (CIA) mouse model, with a focus on its inhibition of synovial hyperplasia, osteoclastogenesis, B cell activation, and joint inflammation. Additionally, through histological analysis and detection of inflammatory markers, we further explored the potential molecular mechanisms of Loxo-305. The results of this study are expected to provide theoretical basis and experimental support for novel therapeutic strategies in RA.

Materials and Methods

Establishment of RA Mice Model

Forty male Dilute Brown Non-Agouti 1 (DBA/1) mice (6–8 weeks old, 25 $\pm$ 2 g) were purchased from GENETMED (Changchun, China). The mice were housed in a specific pathogen-free (SPF) environment under controlled conditions: a 12-hour light/dark cycle, temperature of 22 $\pm$ 2 °C, and relative humidity of 50 $\pm$ 10%. All mice had free access to standard rodent chow and water. The establishment of the RA mouse model was based on the study by Tu *et al.* [22]. The 40 mice were randomly divided into four groups (control group, model group, low Loxo-305 group, high Loxo-305 group), with 10 mice in each group. Type II collagen (CC052, Merck, Darmstadt, Germany) was dissolved in 0.1 M acetic acid solution, usually conducted in an ice bath to prevent collagen denaturation. The final concentration was approximately 2 mg/mL. Equal volumes of Complete Freund's Adjuvant (CFA) (P2036, Beyotime, Shanghai, China) were mixed with the dissolved collagen (1:1 volume ratio) to form a stable emulsion. The mice in the model group, low Loxo-305 group, and high Loxo-305 group were injected with 100 µL of the emulsion via the tail vein. Clinical symptoms of arthritis were observed 2 weeks after immunization. The severity of RA was assessed by scoring the degree of swelling in each joint. We defined successful model construction as the development of visible and measurable joint swelling and stiffness in at least one limb within 2 weeks after immunization, following the criteria described by Tu *et al.* [22]. The degree of joint swelling was scored using a standardized clinical scoring system Swollen Joint Count (SJC), with a score ranging from 0 to 4 for each limb (a maximum total score of 16 per mouse). The evaluation criteria of this system include joint redness, swelling, and deformity. Mice with a total score of $\geq$6 were considered to have successfully developed RA. The overall success rate of model induction was approximately 85%.

Drug Treatment

Regarding the dosing of Loxo-305 (HY-131328, MedChemExpress, NJ, USA), the concentrations of 10 mg/kg/day and 20 mg/kg/day were selected based on findings obtained from preliminary experiments in mouse models, to ensure both safety and therapeutic relevance. The mice in the model group and the control group, which were healthy animals, received daily subcutaneous injections of an equal volume of normal saline as administered to the low- and high-dose groups. The mice in the low Loxo-305 group received subcutaneous injections of Loxo-305 at a dose of 10 mg/kg/day, whereas the mice in the high Loxo-305 group received subcutaneous injections of Loxo-305 at a dose of 20 mg/kg/day. The treatment period lasted for 2 weeks. After 2 weeks, the mice were euthanized by cervical dislocation, and their peripheral blood and joint tissues

were collected for analysis. To minimize bias, all histological evaluations, including hematoxylin and eosin (HE) and tartrate-resistant acid phosphatase (TRAP) staining, were performed under blinded conditions by two independent investigators who were unaware of the group assignments. Scoring was conducted based on a predefined standardized scoring system (Histological Score for Arthritis or Osteoclast Number/Surface per Bone Perimeter) to ensure objectivity and consistency. This study has been approved by the Ethics Committee of the Shandong Provincial Hospital Affiliated to Shandong First Medical University (NO.2025-033). All experimental procedures were conducted in strict accordance with the Regulations for the Administration of Laboratory Animals and the NIH Guide for the Care and Use of Laboratory Animals.

Hematoxylin and Eosin Staining

The hind limbs of mice were fixed in tissue fixative for 24 hours. After dehydration in a series of ethanol solutions of varying concentrations, the tissues were cleared and embedded in paraffin. The tissue sections were cut at a thickness of 5 µm, followed by deparaffinization and rehydration. Subsequently, HE staining (C0105S, Beyotime, Shanghai, China) was performed. After staining, the sections were dehydrated through a series of ethanol and then cleared. The slides were then mounted, and the morphological changes in the joint tissue were observed and assessed under a microscope (BX53, Olympus, Tokyo, Japan). Reference for histological scoring of inflammatory tissues by HE staining [23]. Pannus formation was scored from 0 to 3 (0 = none, 1 = mild, 2 = moderate, 3 = extensive pannus invasion into cartilage or bone). Cell infiltration was scored from 0 to 3 based on the density of inflammatory cells (0 = none, 1 = mild, 2 = moderate, 3 = severe). Synovial hyperplasia was scored from 0 to 3 according to the thickness of the synovial lining (0 = 1–2 layers, 1 = 3–4 layers, 2 = 5–6 layers, 3 = >6 layers). Cartilage erosion was scored from 0 to 3 (0 = no damage, 1 = superficial erosion, 2 = moderate erosion, 3 = severe erosion involving deep cartilage or subchondral bone). All histological assessments were performed, in a blinded manner, by two independent observers to ensure objectivity and reproducibility.

TRAP Staining

The joint tissue was dissected and fixed in fixative solution. After dehydration in a series of ethanol solutions of varying concentrations, the tissue was cleared and embedded in paraffin. The tissue sections were cut at a thickness of 5 µm. The paraffin sections were deparaffinized, followed by rehydration in a series of ethanol solutions of decreasing concentrations (100%, 95%, 75%) and rinsing with distilled water. The sections were then immersed in staining solution from the TRAP staining kit (HK2041, HaoKebio, Hangzhou, China). Excess staining solution was removed by rinsing the sections with distilled water. The sections were mounted and observed under a microscope (BX53, Olympus, Tokyo, Japan).

Immunohistochemistry

The synovial tissue was fixed in tissue fixative. Dehydration of the tissue was performed using a series of ethanol solutions, followed by clearing with xylene. After clearing, the tissue was embedded in paraffin and sectioned into 5 µm thick slices. Dewaxing was conducted using xylene, followed by rehydration in ethanol. Antigen retrieval was performed using citrate buffer in a heat-induced method. Nonspecific binding sites were blocked with normal serum. The tissue was incubated with a specific primary antibody (Cluster of Differentiation 19 (CD19) [1:500, ab245235, Abcam, Cambridge, UK], Receptor Activator of Nuclear Factor Kappa-B Ligand (RANKL) [1:500, ab9957, Abcam, Cambridge, UK], CD11b [1:500, ab133357, Abcam, Cambridge, UK]) for 1 hour. After washing, the tissue was incubated with a Horseradish Peroxidase (HRP)-conjugated secondary antibody (1:500, ab6721, Abcam, Cambridge, UK). 3,3′-Diaminobenzidine (DAB) was used for color development. Hematoxylin counterstaining was then performed. Finally, the tissue was mounted with mounting medium and observed under a microscope.

B Cell Differentiation Stimulation of Spleen Cells

The Mycoplasma test results for the activated B cells in this section were negative. Spleen tissue from mice of different treatment groups was collected and placed into sterile phosphate-buffered saline (PBS). The spleen cells were then isolated using a mesh filter. Red blood cells were removed using red blood cell lysis buffer to obtain a purified single-cell suspension. The spleen cell suspension was filtered to remove larger tissue chunks, in order to produce a single-cell suspension. The cells were washed with PBS to ensure no impurities remained. The spleen cell suspension was treated with anti-immunoglobulin M (IgM) antibody (10 µg/mL; ab212201, Abcam, Cambridge, UK) and incubated at 37 °C with 5% CO_2 for 1 hour. After stimulation, the cells were further cultured in RPMI-1640 medium (11875101, Gibco, Waltham, MA, USA) supplemented with 10% fetal bovine serum (FBS; FB12999102, Gibco, Waltham, MA, USA) and 1% penicillin/streptomycin (15-140-148, Gibco, Waltham, MA, USA). During this process, B cells were activated and began to proliferate.

EdU Staining

In this study, 5-ethynyl-2′-deoxyuridine (EdU) staining was performed using a commercial EdU fluorescence staining kit (C0081L, Beyotime, Shanghai, China). First, the cells were seeded into an appropriate culture plate and allowed to grow to a density of 10^5 cells. Then, 10 µM EdU was added to the culture medium and incubated for 1 hour to allow incorporation into the newly synthesized DNA strands. Next, the cells were fixed for 10 minutes

and washed. Afterward, the cells were permeabilized for 10 minutes and subjected to another round of washing. Upon the addition of EdU reaction solution, the cells were incubated for 30 minutes, followed by washing. The cell nuclei were stained with 4′,6-diamidino-2-phenylindole (DAPI) and incubated for 15 minutes. After washing and mounting with coverslips, the cells were observed under a fluorescence microscope (BX53, Olympus, Tokyo, Japan).

Flow Cytometry

A single-cell suspension containing mouse spleen cells, prepared according to the above-mentioned steps, was centrifuged at 400 rpm. Following washing, the cells were resuspended in Fluorescence-Activated Cell Sorting (FACS) buffer. The cell suspension was adjusted to a density of 1×10^6 cells/mL. The cells were incubated in the dark at 4 °C for 30 minutes. Then, specific antibodies—typically fluorescence-labeled primary antibodies against CD69 (1:1000, ab307081, Abcam, Cambridge, UK), CD19 (1:1000, ab245235, Abcam, Cambridge, UK), CD86 (1:1000, ab239075, Abcam, Cambridge, UK), CD138 (1:1000, ab128936, Abcam, Cambridge, UK), and B220 (1:1000, ab283506, Abcam, Cambridge, UK)—were added to the cell suspension. Following incubation in the dark at 4 °C for 30 minutes, the cells were washed three times with FACS buffer to remove unbound antibodies. Finally, the processed cells were analyzed using a flow cytometer (MoFlo Astrios, Beckman Coulter, Indianapolis, IN, USA).

Enzyme-linked Immunosorbent Assay

For this experiment, commercial enzyme-linked immunosorbent assay (ELISA) kits for total IgG (PI480), IgG1 (PI458), IgG2a (ab133046), RANKL (ab269553), IL-6 (PI326), TNF-α (PT512), and IL-1β (PI301) were purchased from Beyotime (Shanghai, China) and Abcam (Cambridge, UK). Serum samples were diluted according to the instructions provided in the kit manual. Standards corresponding to a range of different concentrations were prepared using the sample diluent. The standards and samples (100 µL per well) were added to the wells of the microplate. After sealing with sealing film, the microplate was incubated at 37 °C for 1 hour, according to the kit instructions. After incubation and liquid removal from each well, the plate was washed three times with washing buffer. Next, enzyme conjugate was added to each well. The plate was incubated at 37 °C for 30 minutes. After incubation, the washing steps were repeated. To each well, 100 µL of substrate solution was added to initiate the reaction, which was allowed to proceed in the dark at room temperature until the wells containing standards showed a detectable color intensity, at which point 100 µL of stop solution was added to each well, causing the color to turn yellow. Absorbance was measured at 450 nm wavelength using a microplate reader (Epoch 2, BioTek, Winooski, VT, USA).

Quantitative Real-time Polymerase Chain Reaction (qRT-PCR)

First, total RNA was extracted from tissue or cell samples using an RNA extraction kit (R0077S, Beyotime, Shanghai, China). Then, using a reverse transcription kit (D7168S, Beyotime, Shanghai, China), we reverse-transcribed 1 µg of RNA into cDNA, with the reverse transcription conditions set at 42 °C for 60 minutes, followed by heating at 72 °C to terminate the reaction. Next, the qPCR reaction system was prepared, including the cDNA template, specific primers, qPCR Master Mix, etc., with a final reaction volume of 20 µL. The mixture was added to reaction tubes or a 96-well plate, and the qPCR program was set as follows: 95 °C for 5 minutes for pre-denaturation, followed by 40 cycles of 95 °C for 15 seconds (denaturation) and 60 °C for 30 seconds (annealing/extension), along with a melting curve analysis to confirm product specificity. During each annealing/extension phase, qPCR signals in the form of fluorescence were detected. Relative expression of target genes was calculated using the $\Delta\Delta$Ct method. ΔCt represents the difference in Ct values between the target gene and the internal control gene, while $\Delta\Delta$Ct represents the difference in ΔCt between the experimental group and the control group. The final relative expression was calculated using this formula: $2^{-\Delta\Delta Ct}$. A stably expressed internal control gene (β-actin) was used for normalization. The primer sequences used in this study are listed in Table 1.

Statistical Analysis

Experimental data were analyzed using GraphPad Prism software (version 9.0, GraphPad Software, Inc., San Diego, CA, USA). Results are expressed as mean ± standard deviation (SD). Group comparisons were achieved using a *t*-test, while one-way analysis of variance (ANOVA)

Table 1. Sequences of primers used in this work.

Primer name	Primer sequence (5′ to 3′)
Mus-TRAP-F	CACTCCCACCCTGAGATTTGT
Mus-TRAP-R	CATCGTCTGCACGGTTCTG
Mus-DC-STAMP-F	TCCTCCATGAACAAACAGTTCCAA
Mus-DC-STAMP-R	AGACGTGGTTTAGGAATGCAGCTC
Mus-CTSK-F	GAAGAAGACTCACCAGAAGCAG
Mus-CTSK-R	TCCAGGTTATGGGCAGAGATT
Mus-RANKL-F	CAGCATCGCTCTGTTCCTGTA
Mus-RANKL-R	CTGCGTTTTCATGGAGTCTCA
Mus-OPG-F	ACCCAGAAACTGGTCATCAGC
Mus-OPG-R	CTGCAATACACACACTCATCACT
Mus-β-actin-F	GGCTGTATTCCCCTCCATCG
Mus-β-actin-R	CCAGTTGGTAACAATGCCATGT

Note: F, forward; R, reverse; TRAP, tartrate-resistant acid phosphatase; DC-STAMP, Dendritic Cell-Specific Transmembrane Protein; CTSK, Cathepsin K; RANKL, Receptor Activator of Nuclear Factor Kappa-B Ligand; OPG, Osteoprotegerin.

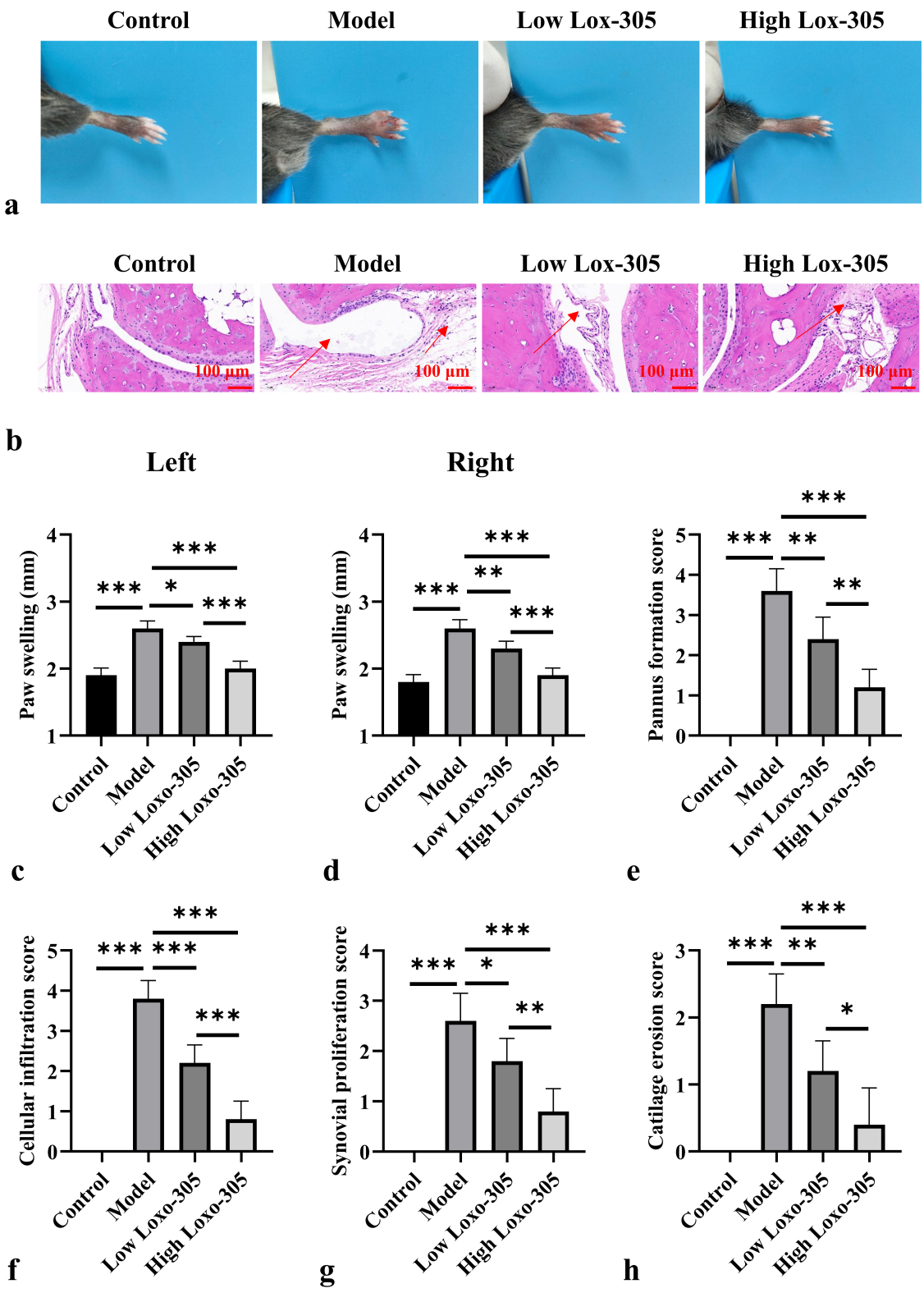

Fig. 1. Loxo-305 effectively abrogates the progression of RA in mice. (a) Representative images of RA mouse paws. (b) Representative HE-stained images of mouse ankle joint sections. The red arrow indicates the area of inflammation and destruction in the synovial tissue of the joint. (c,d) Measurement of paw swelling thickness in the left and right paws at the end of the study. (e–h) Histological scores for pannus formation, cell infiltration, synovial hyperplasia, and cartilage erosion in the ankle joints. $n = 10$. *$p < 0.05$, **$p < 0.01$, ***$p < 0.001$. Abbreviations: HE, hematoxylin and eosin; RA, Rheumatoid arthritis.

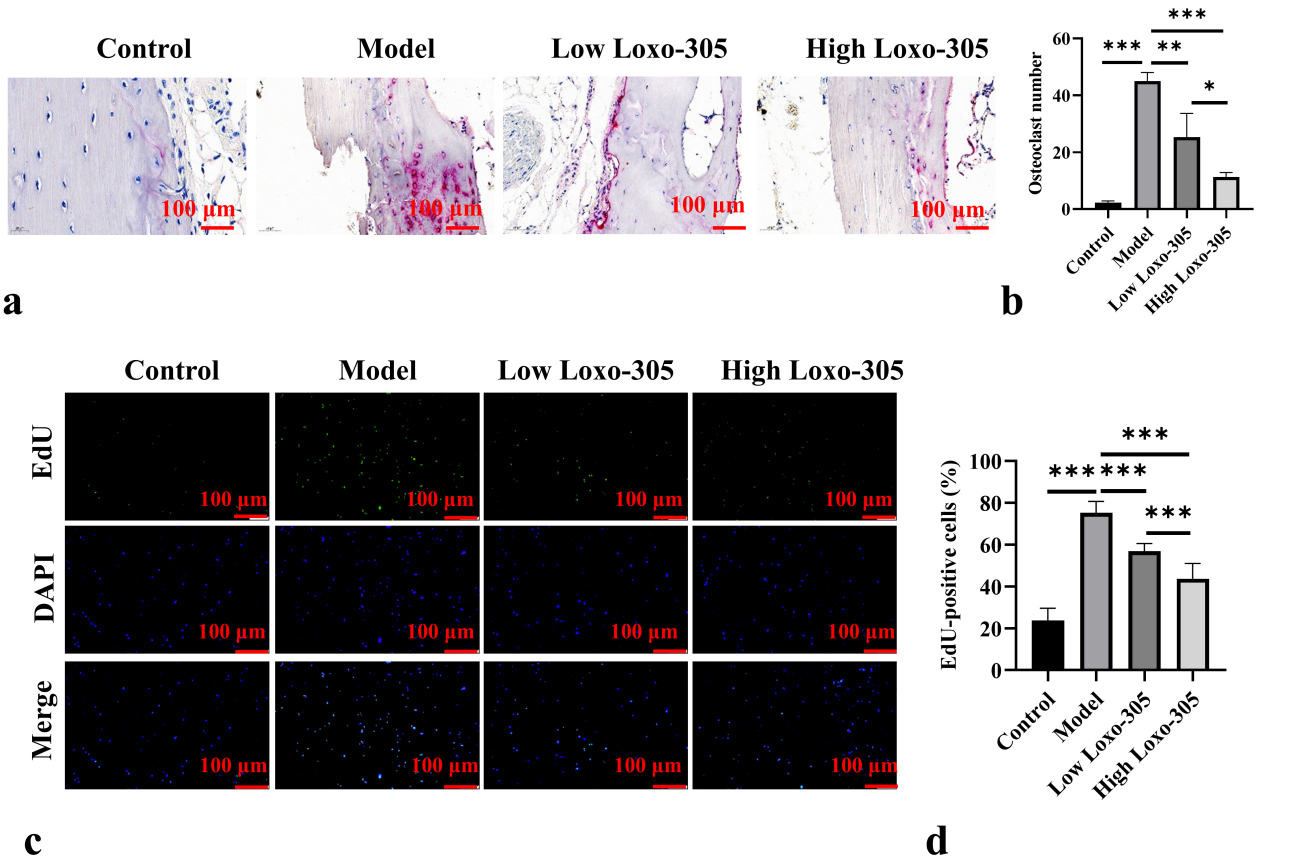

Fig. 2. Loxo-305 reduces osteoclastogenesis and B cell activation in RA mice. (a,b) Representative TRAP staining images of inflamed joints in hind paws from different groups of mice and quantitative results of TRAP-positive osteoclasts. (c,d) B cell activity was assessed using EdU staining after splenocytes isolated from different treatment groups were stimulated with anti-IgM (10 μg/mL) to activate B cells. $n = 10$. *$p < 0.05$, **$p < 0.01$, ***$p < 0.001$. Abbreviation: RA, Rheumatoid arthritis; EdU, 5-ethynyl-2′-deoxyuridine; IgM, immunoglobulin M; DAPI, 4′,6-diamidino-2-phenylindole.

with Tukey's post hoc test was applied for multi-group analyses. Results with $p < 0.05$ were considered statistically significant.

Results

Loxo-305 Effectively Abrogates the Progression of RA in Mice

Paw images of RA mice (Fig. 1a) show that Loxo-305 administration significantly improves disease progression in a dose-dependent manner. Based on the HE staining results (Fig. 1b), compared to the control group, the model group exhibited an increased number of synovial cell layers, tissue expansion, severe inflammatory cell infiltration, uneven cartilage staining, thinning or loss of cartilage layers, irregular cartilage matrix, and areas of bone destruction (shown by lighter, irregular staining and erosion of trabecular bone structure). Additionally, neovascularization was observed, with the vessel walls showing deeper staining. Loxo-305 administration significantly improved these pathological changes. Loxo-305 significantly reduced paw swelling in RA mice ($p < 0.05$, Fig. 1c,d). Compared to the control group, the model group had significantly increased histological scores for pannus formation, cell infiltration, synovial hyperplasia, and cartilage erosion ($p < 0.05$, Fig. 1e–h) while Loxo-305 treatment at different doses significantly reduced these scores in RA mice ($p < 0.05$). Moreover, the high-dose Loxo-305 group exhibited superior therapeutic effects compared to the low-dose group.

Loxo-305 Reduces Osteoclastogenesis and B Cell Activation in RA Mice

First, we identified osteoclasts in inflamed joints using TRAP staining. The number of osteoclasts significantly increased in the RA model group ($p < 0.05$, Fig. 2a,b), while different doses of Loxo-305 significantly reduced osteoclastogenesis ($p < 0.05$). Loxo-305 dose-dependently inhibited the proliferation of splenic B cells in RA mice (Fig. 2c,d). Compared to the control group, the number of

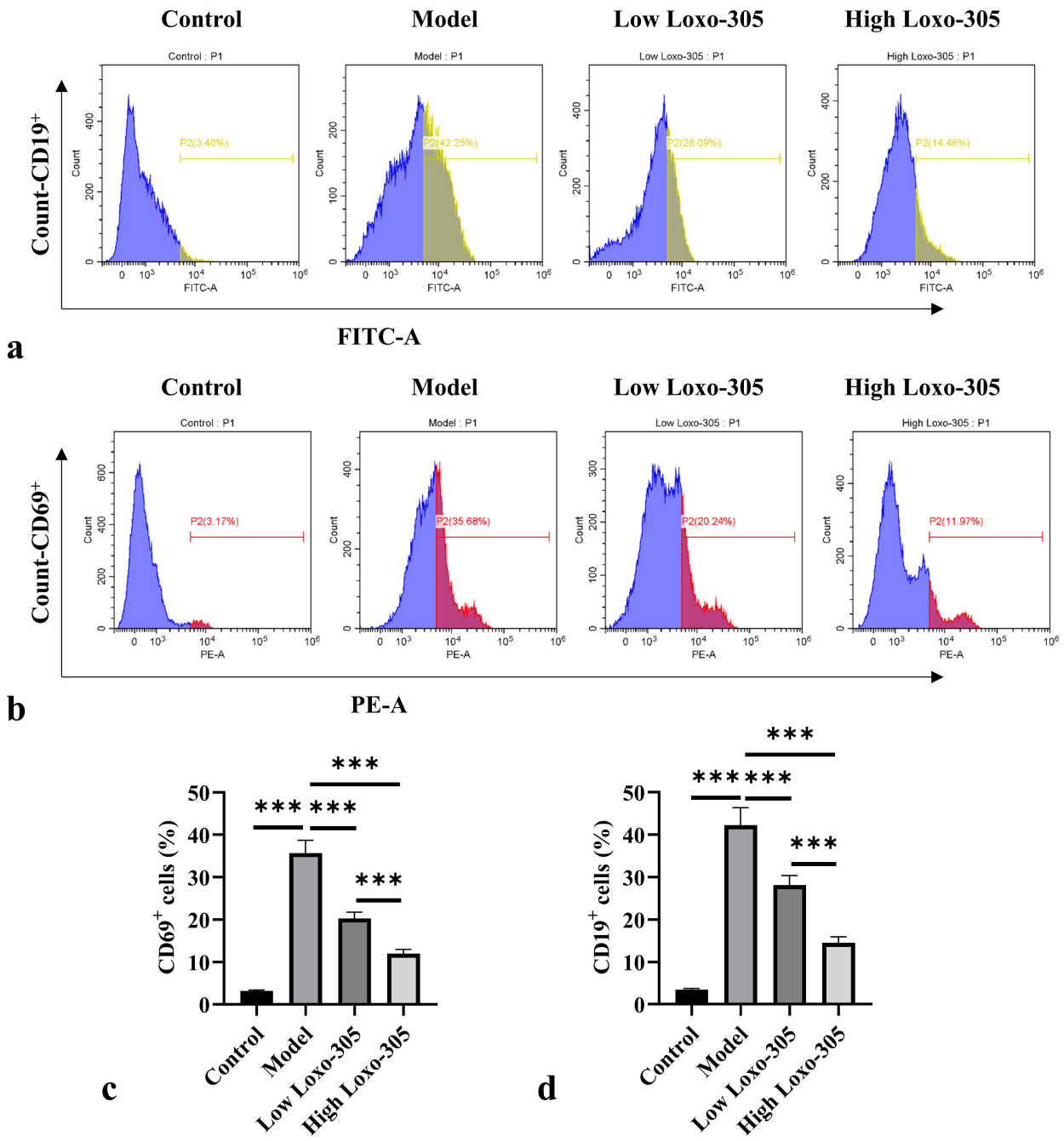

Fig. 3. Loxo-305 inhibits B cell activation in RA mice. The positive expression of $CD19^+$ (a,d) and $CD69^+$ (b,c) in splenocytes was measured by means of flow cytometry. $n = 10$. $^{***}p < 0.001$. Abbreviation: RA, Rheumatoid arthritis; CD19, Cluster of Differentiation 19; PE-A, Phycoerythrin-Area; FITC-A, Fluorescein Isothiocyanate-Area.

EdU-positive B cells in the spleens of the model group was significantly higher, while Loxo-305 treatment at different doses significantly reduced the number of EdU-positive cells ($p < 0.05$). $CD69^+$ $CD19^+$ positive expression in splenic B cells was significantly increased in the model group, while both low and high doses of Loxo-305 significantly decreased $CD69^+$ $CD19^+$ positive expression ($p < 0.05$, Fig. 3a–d). $CD86^+$ $CD19^+$ positive expression in splenic B cells was significantly elevated in the model group, while Loxo-305 treatment at both doses significantly reduced $CD86^+$ $CD19^+$ positive expression ($p < 0.05$, Fig. 4a–d). Moreover, high-dose Loxo-305 treatment showed a more pronounced effect in reducing osteoclastogenesis and B cell activation in RA mice compared to those receiving low-dose Loxo-305.

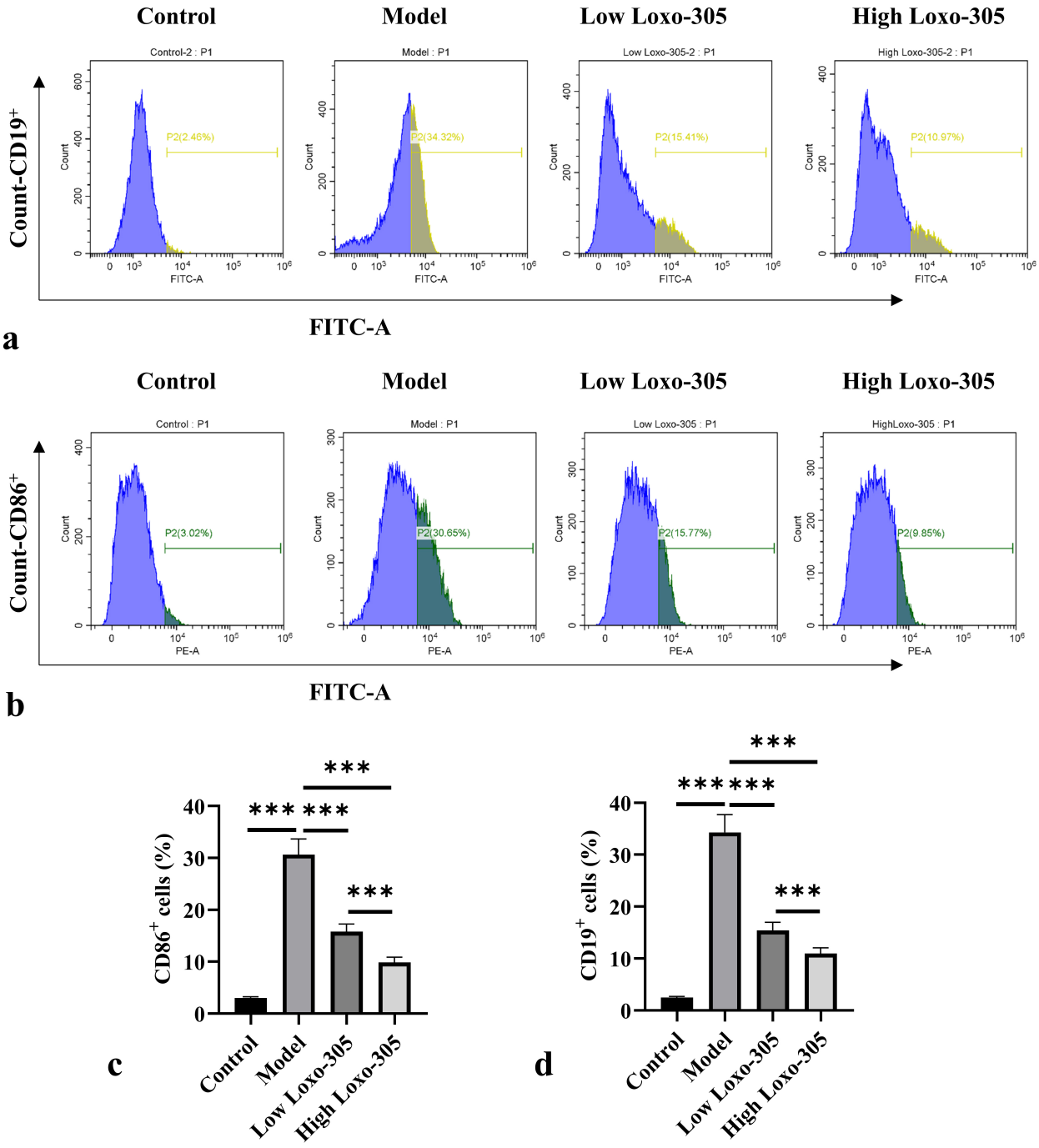

Fig. 4. Loxo-305 inhibits B cell activation in RA mice. The positive expression of $CD19^+$ (a,d) and $CD86^+$ (b,c) in splenocytes was measured by means of flow cytometry. $n = 10$. $^{***}p < 0.001$. Abbreviation: RA, Rheumatoid arthritis.

Loxo-305 Inhibits Plasma Cell and Autoantibody Production in RA Mice

Next, we analyzed the proportion of plasma cells in the spleen. As shown in Fig. 5a–d, the positive expression of $CD138^+$ $B220^+$ in the spleens of mice in the model group was significantly increased compared to the control group, while Loxo-305 treatment significantly inhibited the expression of $CD138^+$ $B220^+$ ($p < 0.05$). This indicates that Loxo-305 significantly suppresses plasma cell production. The serum levels of total IgG, IgG1, and IgG2a in the mice of model group were significantly higher than those control group, while Loxo-305 treatment significantly reduced the serum levels of total IgG, IgG1, and IgG2a in the RA mice compared to those of model group ($p < 0.05$, Fig. 5e–g).

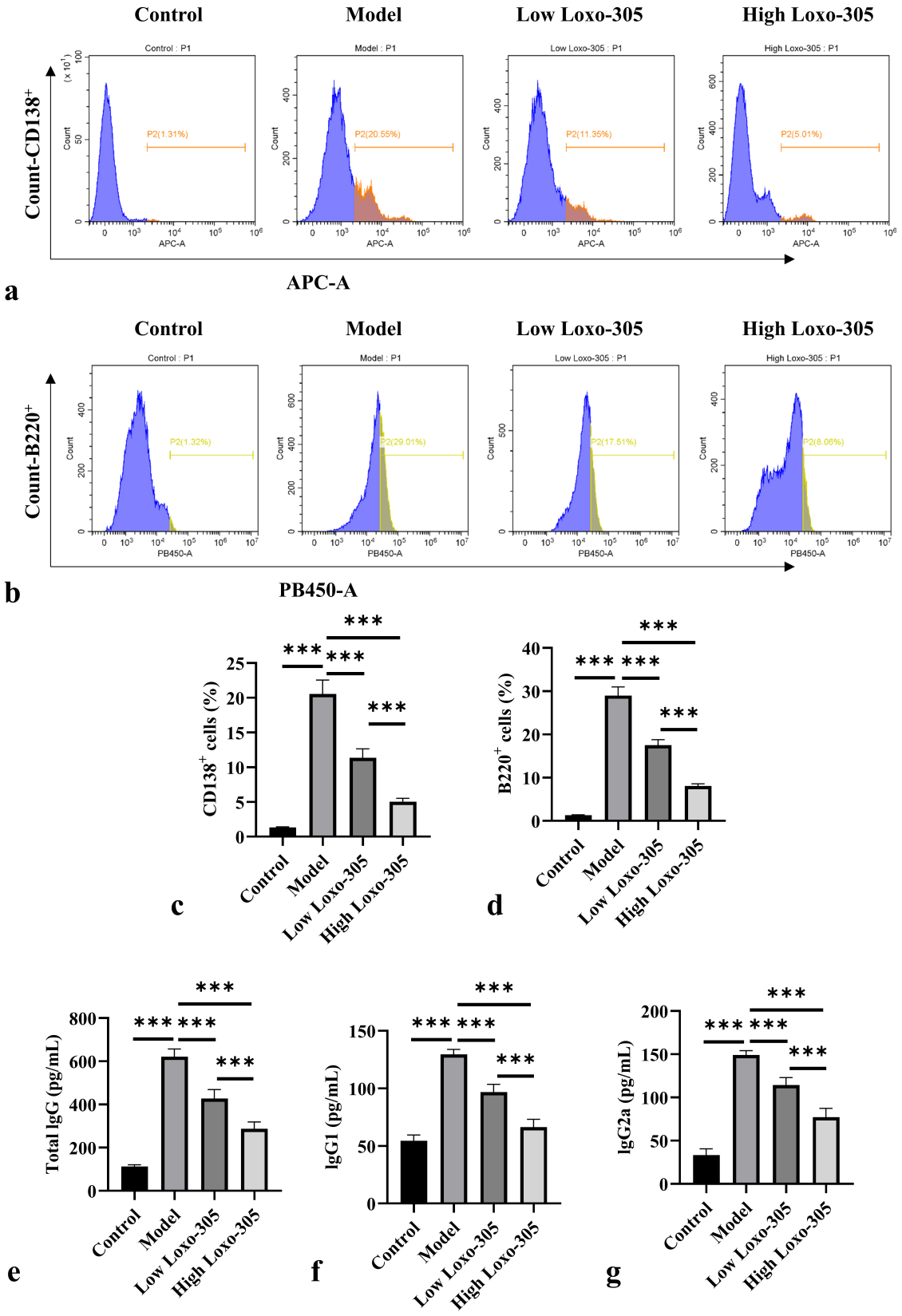

Fig. 5. Loxo-305 inhibits plasma cell and autoantibody production in RA mice. (a–d) Flow cytometry analysis of $CD138^+$ (a,c) and $B220^+$ (b,d) expression in spleen cells. (e–g) ELISA measurement of total IgG, IgG1, and IgG2a levels in mouse serum. $n = 10$. ***$p < 0.001$. Abbreviations: ELISA, enzyme-linked immunosorbent assay; RA, Rheumatoid arthritis.

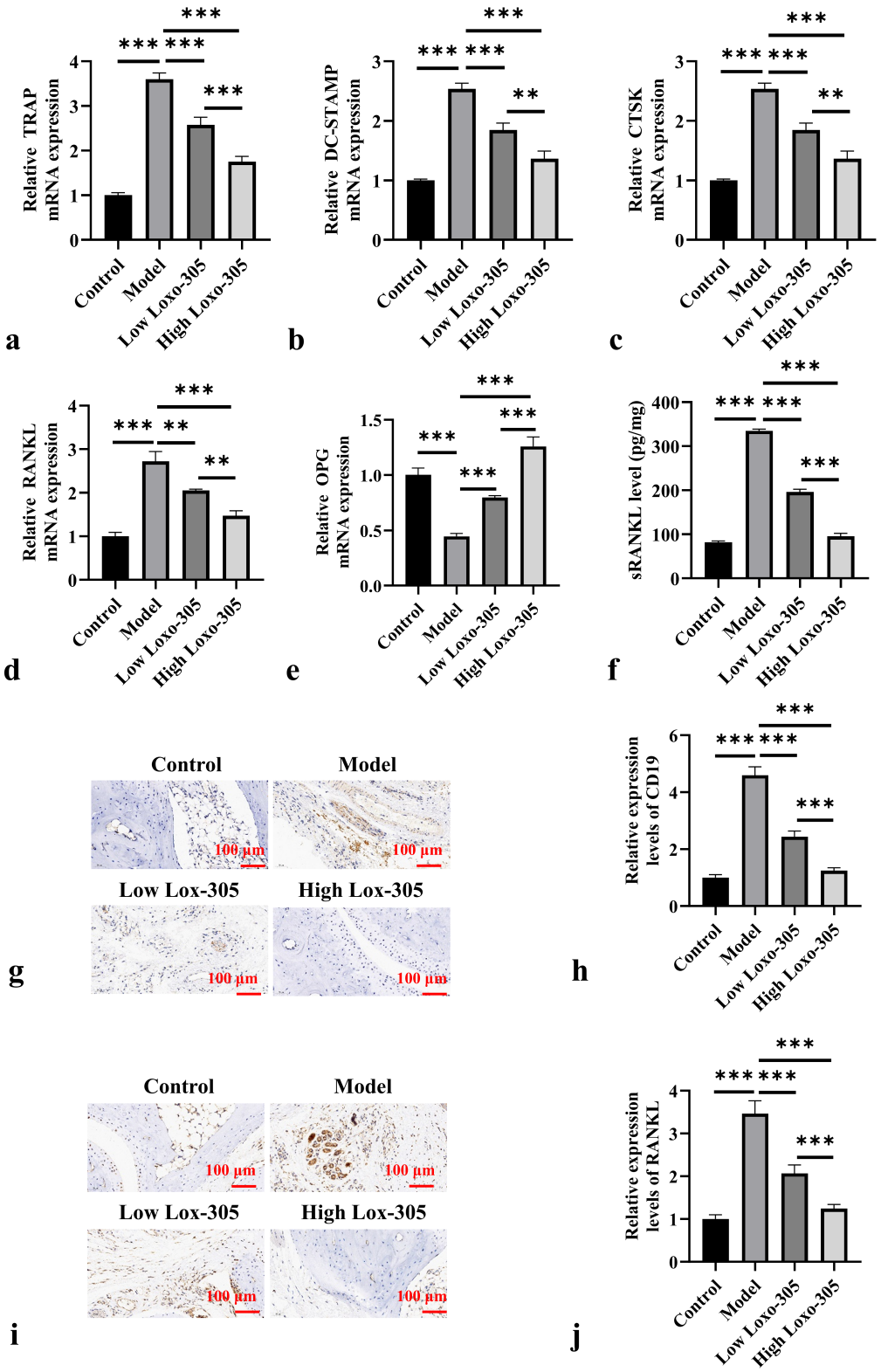

Fig. 6. Loxo-305 reduces osteoclast formation and inhibits RANKL expression. (a–e) mRNA expression levels of TRAP, DC-STAMP, CTSK, RANKL and OPG in mouse joint tissues. (f) ELISA measurement of sRANKL levels in serum from each group. (g,h) Immunohistochemical detection of CD19 expression in joint tissues from each group. (i,j) Immunohistochemical detection of RANKL expression in joint tissues from each group. $n = 10$. $^{**}p < 0.01$, $^{***}p < 0.001$. Abbreviation: ELISA, enzyme-linked immunosorbent assay.

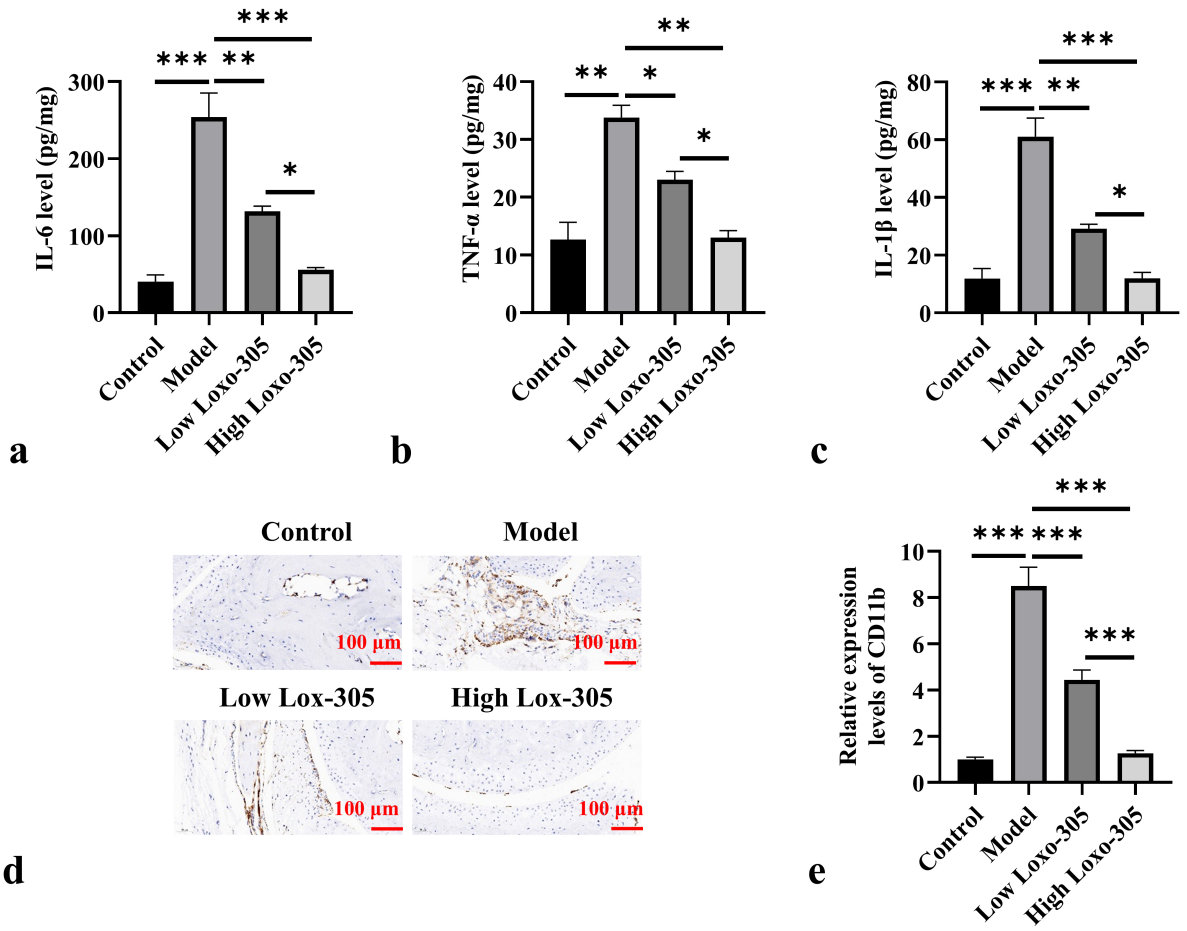

Fig. 7. Loxo-305 inhibits the development of inflammation in joint tissues. (a–c) ELISA measurement of IL-6, TNF-α, and IL-1β levels in serum from each group. (d,e) Immunohistochemical determination of CD11b expression in joint tissues. $n = 10$. *$p < 0.05$, **$p < 0.01$, ***$p < 0.001$. Abbreviations: ELISA, enzyme-linked immunosorbent assay; IL, interleukin; TNF-α, tumor necrosis factor alpha.

Loxo-305 Reduces Osteoclast Formation and Inhibits RANKL Expression

We measured the mRNA levels of TRAP, Dendritic Cell-Specific Transmembrane Protein (DC-STAMP), Cathepsin K (CTSK), RANKL and Osteoprotegerin (OPG) in joint tissues. The mRNA expression levels of TRAP, DC-STAMP, CTSK, and RANKL were significantly higher in the model group compared to the control group, while the mRNA expression levels of these markers were significantly lower in the high- and low-dose Loxo-305 treatment groups compared to the model group ($p < 0.05$, Fig. 6a–d). The mRNA levels of OPG were significantly lower in the model group compared to the control group, while both low and high doses of Loxo-305 treatment significantly increased the mRNA levels of OPG in RA mice ($p < 0.05$, Fig. 6e). The level of sRANKL in peripheral blood from RA mice was very high ($p < 0.05$), and Loxo-305 treatment significantly reduced the sRANKL content in peripheral blood ($p < 0.05$, Fig. 6f). We also performed immunohistochemical analysis to determine the expression of CD19 and RANKL in joint tissues of mice. The results in Fig. 6g–j show that the expression levels of CD19 and RANKL in joint tissues of the model group were significantly higher than those in the control group, and Loxo-305 treatment significantly reduced the expression of CD19 and RANKL in joint tissues of RA model mice ($p < 0.05$). High-dose Loxo-305 treatment is more effective than low-dose treatment in reducing osteoclast formation and inhibiting RANKL expression.

Loxo-305 Inhibits the Development of Inflammation in Joint Tissues

The levels of IL-6, TNF-α, and IL-1β in joint tissues of mice in the model group were significantly higher than those in the control group (Fig. 7a–c). Compared to the model group, the joints of mice receiving Loxo-305 treatment exhibited significantly reduced levels of IL-6, TNF-α, and IL-1β ($p < 0.05$). Additionally, immunohistochemical approach was employed to assess the expression of CD11b in joint tissues. The level of CD11b in the model group was

significantly higher than in the control group (Fig. 7d,e). Compared to the model group, both low- and high-dose Loxo-305 reduced CD11b expression to varying degrees ($p < 0.05$), with the high-dose group showing a more significant reduction ($p < 0.05$).

Discussion

The primary aim of this study was to explore the therapeutic effects of Loxo-305 on the RA mouse model. Our results showed that it not only significantly improved disease progression in a dose-dependent manner, but also exhibited significant inhibitory effects on pathological changes in joint tissues, bone destruction, B cell and plasma cell activation, osteoclastogenesis, and levels of inflammatory factor. The following provides a more in-depth discussion and expansion from multiple perspectives.

The present study showed that Loxo-305 significantly improves joint lesions and tissue damage in RA mice in a dose-dependent manner. High-dose Loxo-305 treatment was particularly effective in reducing synovial hyperplasia, cartilage erosion, and pannus formation. These results are consistent with recent study on the dose-dependent effects of BTK inhibitors, suggesting that higher doses of BTK inhibitors can more effectively block the core immune responses involved in the pathogenesis of RA [24]. Furthermore, the findings of this study imply the critical role of BTK in regulating the pathological development of RA, highlighting the importance of further research on the optimization of BTK inhibitor dosing for clinical application in RA.

In this study, we observed that a subset of plasma cells maintained high levels of B220 expression, which appears to differ from the classical phenotype of mature plasma cells, typically characterized by high CD138 and low or absent B220 expression. This discrepancy can be explained by the activation stage of the analyzed cells. Previous study has shown that during the early or transitional stages of plasma cell differentiation, cells may transiently co-express both B220 and CD138 before they mature into long-lived plasma cells, a growth stage at which B220 expression is ultimately downregulated [25]. This transitional phenotype is particularly evident under conditions of acute activation or *ex vivo* stimulation, where B cell activation gives rise to a heterogeneous population including activated B cells, plasmablasts, and early plasma cell precursors.

Additionally, the immunological microenvironment and pathological context of RA may also influence surface marker expression. Chronic inflammation and changes in the cytokine profile—such as elevated levels of IL-6 and TNF-α observed in RA—can affect B cell fate decisions and phenotypic plasticity, potentially sustaining B220 expression in some plasma cells. Therefore, the high B220 expression observed in our experimental system may reflect this dynamic and complex continuum of differentiation, rather than solely representing terminally differentiated plasma cells.

One of the key pathological features of RA is the overactivation of osteoclasts, which leads to bone destruction and joint dysfunction. Loxo-305 significantly inhibits bone destruction in RA mice by reducing osteoclastogenesis, and it restores the balance of osteoclastogenesis by downregulating RANKL and upregulating OPG expression. This is consistent with previous studies, which indicate that the RANKL/OPG signaling pathway plays a crucial role in regulating osteoclast differentiation and activation [26,27]. Notably, this study showed that Loxo-305 not only effectively reduces RANKL expression in RA joint tissues but also directly affects osteoclast differentiation and function by inhibiting the expression of osteoclast-specific genes such as TRAP, DC-STAMP, and CTSK. These results provide a new therapeutic approach for bone protection in RA patients and further support the potential application of BTK inhibitors in combating bone destruction.

Abnormal activation of B cells is one of the key factors in the pathogenesis of RA, an autoimmune disease mediated by B cells. In this study, Loxo-305 significantly reduced the activation and proliferation of splenic B cells in RA mice and inhibited the expression of B cell activation markers CD69 and CD86, indicating that Loxo-305 effectively suppresses B cell activation. This result is consistent with previous study on the mechanism by which BTK inhibitors regulate B cell function. BTK plays a key role in the B cell receptor signaling pathway, influencing B cell proliferation, activation, and differentiation [28]. Furthermore, Loxo-305 also significantly inhibited the generation of plasma cells and the production of autoantibodies in RA mice, particularly reducing the levels of total IgG, IgG1, and IgG2a, further suggesting that BTK inhibitors can alleviate the immunopathological response of RA by modulating B cell function.

In this study, the selective BTK inhibitor Loxo-305 significantly downregulated the expression of TRAP, DC-STAMP, and CTSK in the joint tissues of CIA mice, suggesting that BTK inhibition may suppress osteoclast differentiation and function by interfering with the RANKL-BTK-Nuclear Factor of Activated T Cells, cytoplasmic 1 (NFATc1) signaling pathway. Among these markers, TRAP is a classical indicator of osteoclast activity, DC-STAMP plays a critical role in the fusion of mononuclear precursors into multinucleated osteoclasts, and CTSK is a key enzyme involved in bone matrix degradation. The coordinated downregulation of these three genes indicates that Loxo-305 may effectively inhibit both osteoclast formation and their bone-resorptive function. One of the pathological features of RA is the inflammatory response in joint tissues, with inflammatory factors such as IL-6, TNF-α, and IL-1β playing a crucial role in the pathogenesis of RA. In this study, Loxo-305 significantly inhibited the expression of these key inflammatory factors in the joint tissues of RA

mice, and reduced macrophage activation by suppressing CD11b expression. Therefore, Loxo-305, as a novel multi-target BTK inhibitor, provides a new potential strategy for the comprehensive treatment of RA.

Although this study primarily focuses on the effects of Loxo-305 in the RA mouse model, it may also have broad applications in other immune-mediated diseases [29,30]. Since Loxo-305 can broadly regulate B cell activation, osteoclastogenesis, and the expression of inflammatory factors, future research could further explore its therapeutic effects in other immune-related diseases and assess its long-term safety and efficacy.

Although this study demonstrates the significant therapeutic effects of Loxo-305 in the RA mouse model, there are still some limitations. First, despite the dose-dependent effect of Loxo-305 observed, the specific dose-response relationship and the optimal therapeutic dose still require further optimization. Second, this study primarily focuses on the short-term effects of Loxo-305 in the RA mouse model, and the efficacy and potential side effects of long-term use of Loxo-305 need to be confirmed through further experimental and clinical research. Additionally, although this study revealed the regulatory effects of Loxo-305 on immune cells such as B cells and osteoclasts, its impact on other immune cell types, such as T cells and natural killer cells, remains unclear, which will be one of the key directions for future research.

Recent clinical-stage BTK inhibitors such as fenebrutinib and evobrutinib have shown promising efficacy in autoimmune diseases including RA, primarily by targeting B cell signaling and reducing inflammatory cytokine levels. However, their clinical use has been limited by issues such as off-target effects, variable efficacy, and safety concerns, including risks of infection and hepatotoxicity in long-term treatment. In contrast, Loxo-305 is a next-generation, highly selective BTK inhibitor with minimal off-target activity, which allows for more precise modulation of B cell function and has a favorable safety profile. Our study demonstrates that Loxo-305 not only significantly reduces B cell and plasma cell activation but also strongly inhibits osteoclastogenesis and joint destruction, effects not consistently observed with earlier BTK inhibitors in preclinical RA models. These findings suggest that Loxo-305 offers a dual advantage of immune regulation and bone protection, positioning it as a potentially superior therapeutic option for RA compared to currently available BTK inhibitors in clinical development. Further comparative studies, including direct head-to-head evaluations with fenebrutinib and evobrutinib in RA models, will be valuable to confirm these advantages and support the translation of Loxo-305 into clinical trials for RA treatment.

In summary, this study showed that Loxo-305 can effectively alleviate the progression of RA in mice by inhibiting B cell activation, osteoclastogenesis, and the expression of inflammatory factors. As a novel BTK inhibitor, Loxo-305 demonstrates broad potential for application in the treatment of RA, and future research could further explore its potential applications in other immune-related diseases.

Conclusions

Loxo-305 significantly attenuates inflammatory response in RA mice and improves pathological changes in joint tissue by inhibiting osteoclastogenesis and reducing the activation of B cells and plasma cells. This novel BTK inhibitor also reduces tissue damage by downregulating the expression of RANKL and inflammatory factors, exhibiting a dose-dependent therapeutic effect. Overall, the present study demonstrated that the high-dose Loxo-305 is more effective than the low-dose agent in improving RA symptoms, highlighting its potential application value in the treatment of RA.

Availability of Data and Materials

The data that support the findings of this study are available from the corresponding author upon reasonable request.

Author Contributions

XNW and AHL designed the research study. XNW, LJC and AHL performed the research. XNW and AHL collected and analyzed the data. XNW, LJC and AHL has been involved in drafting the manuscript and all authors have been involved in revising it critically for important intellectual content. All authors give final approval of the version to be published. All authors have participated sufficiently in the work to take public responsibility for appropriate portions of the content and agreed to be accountable for all aspects of the work in ensuring that questions related to its accuracy or integrity.

Ethics Approval and Consent to Participate

This study was approved by the Ethics Committee of the Shandong Provincial Hospital Affiliated to Shandong First Medical University (NO.2025-033).

Acknowledgment

Not applicable.

Funding

This research received no external funding.

Conflict of Interest

The authors declare no conflict of interest.

References

[1] Brown P, Pratt AG, Hyrich KL. Therapeutic advances in rheumatoid arthritis. BMJ (Clinical Research Ed.). 2024; 384: e070856. https://doi.org/10.1136/bmj-2022-070856.

[2] Chen L, Wu B, Mo L, Chen H, Zhao Y, Tan T, *et al*. Associations between biological ageing and the risk of, genetic susceptibility to, and life expectancy associated with rheumatoid arthritis: a secondary analysis of two observational studies. The Lancet. Healthy Longevity. 2024; 5: e45–e55. https://doi.org/10.1016/S2666-7568(23)00220-9.

[3] Zheng Y, Wei K, Jiang P, Zhao J, Shan Y, Shi Y, *et al*. Macrophage polarization in rheumatoid arthritis: signaling pathways, metabolic reprogramming, and crosstalk with synovial fibroblasts. Frontiers in Immunology. 2024; 15: 1394108. https://doi.org/10.3389/fimmu.2024.1394108.

[4] Qi P, Chen X, Tian J, Zhong K, Qi Z, Li M, *et al*. The gut homeostasis-immune system axis: novel insights into rheumatoid arthritis pathogenesis and treatment. Frontiers in Immunology. 2024; 15: 1482214. https://doi.org/10.3389/fimmu.2024.1482214.

[5] Gan PR, Wu H, Zhu YL, Shu Y, Wei Y. Glycolysis, a driving force of rheumatoid arthritis. International Immunopharmacology. 2024; 132: 111913. https://doi.org/10.1016/j.intimp.2024.111913.

[6] Hu F, Shi L, Liu X, Chen Y, Zhang X, Jia Y, *et al*. Proinflammatory phenotype of B10 and B10pro cells elicited by TNF-α in rheumatoid arthritis. Annals of the Rheumatic Diseases. 2024; 83: 576–588. https://doi.org/10.1136/ard-2023-224878.

[7] Chauhan K, Jandu JS, Brent LH, Al-Dhahir MA. Rheumatoid Arthritis. StatPearls Publishing: Treasure Island (FL). 2024.

[8] Mok TC, Mok CC. Non-TNF biologics and their biosimilars in rheumatoid arthritis. Expert Opinion on Biological Therapy. 2024; 24: 599–613. https://doi.org/10.1080/14712598.2024.2358165.

[9] Favalli EG, Maioli G, Caporali R. Biologics or Janus Kinase Inhibitors in Rheumatoid Arthritis Patients Who are Insufficient Responders to Conventional Anti-Rheumatic Drugs. Drugs. 2024; 84: 877–894. https://doi.org/10.1007/s40265-024-02059-8.

[10] Chen H, Fu X, Wu X, Zhao J, Qiu F, Wang Z, *et al*. Gut microbial metabolite targets HDAC3-FOXK1-interferon axis in fibroblast-like synoviocytes to ameliorate rheumatoid arthritis. Bone Research. 2024; 12: 31. https://doi.org/10.1038/s41413-024-00336-6.

[11] Yang M, Zhu L. Osteoimmunology: The Crosstalk between T Cells, B Cells, and Osteoclasts in Rheumatoid Arthritis. International Journal of Molecular Sciences. 2024; 25: 2688. https://doi.org/10.3390/ijms25052688.

[12] Chang JW, Tang CH. The role of macrophage polarization in rheumatoid arthritis and osteoarthritis: Pathogenesis and therapeutic strategies. International Immunopharmacology. 2024; 142: 113056. https://doi.org/10.1016/j.intimp.2024.113056.

[13] Bucci L, Hagen M, Rothe T, Raimondo MG, Fagni F, Tur C, *et al*. Bispecific T cell engager therapy for refractory rheumatoid arthritis. Nature Medicine. 2024; 30: 1593–1601. https://doi.org/10.1038/s41591-024-02964-1.

[14] Schett G, Nagy G, Krönke G, Mielenz D. B-cell depletion in autoimmune diseases. Annals of the Rheumatic Diseases. 2024; 83: 1409–1420. https://doi.org/10.1136/ard-2024-225727.

[15] Abeles I, Palma C, Meednu N, Payne AS, Looney RJ, Anolik JH. B Cell-Directed Therapy in Autoimmunity. Annual Review of Immunology. 2024; 42: 103–126. https://doi.org/10.1146/annurev-immunol-083122-044829.

[16] Neppelenbroek S, Blomberg NJ, Kampstra ASB, van der Hem JGK, Huizinga TWJ, Toes REM, *et al*. Autoreactive B cells remain active despite clinical disease control in rheumatoid arthritis. Journal of Autoimmunity. 2024; 149: 103320. https://doi.org/10.1016/j.jaut.2024.103320.

[17] De Bondt M, Renders J, Struyf S, Hellings N. Inhibitors of Bruton's tyrosine kinase as emerging therapeutic strategy in autoimmune diseases. Autoimmunity Reviews. 2024; 23: 103532. https://doi.org/10.1016/j.autrev.2024.103532.

[18] Nadeem A, Ahmad SF, Al-Harbi NO, Ibrahim KE, Alqahtani F, Alanazi WA, *et al*. Bruton's tyrosine kinase inhibition attenuates oxidative stress in systemic immune cells and renal compartment during sepsis-induced acute kidney injury in mice. International Immunopharmacology. 2021; 90: 107123. https://doi.org/10.1016/j.intimp.2020.107123.

[19] Cool A, Nong T, Montoya S, Taylor J. BTK inhibitors: past, present, and future. Trends in Pharmacological Sciences. 2024; 45: 691–707. https://doi.org/10.1016/j.tips.2024.06.006.

[20] Schultze MD, Reeves DJ. Pirtobrutinib: A New and Distinctive Treatment Option for B-Cell Malignancies. The Annals of Pharmacotherapy. 2024; 58: 1064–1073. https://doi.org/10.1177/10600280231223737.

[21] Treon SP, Sarosiek S, Castillo JJ. How I use genomics and BTK inhibitors in the treatment of Waldenström macroglobulinemia. Blood. 2024; 143: 1702–1712. https://doi.org/10.1182/blood.2022017235.

[22] Tu J, Chen W, Fang Y, Han D, Chen Y, Jiang H, *et al*. PU.1 promotes development of rheumatoid arthritis via repressing FLT3 in macrophages and fibroblast-like synoviocytes. Annals of the Rheumatic Diseases. 2023; 82: 198–211. https://doi.org/10.1136/ard-2022-222708.

[23] van den Berg WB. Animal models of arthritis. What have we learned? The Journal of Rheumatology. Suppl. 2005; 72: 7–9.

[24] Liu YT, Ding HH, Lin ZM, Wang Q, Chen L, Liu SS, *et al*. A novel tricyclic BTK inhibitor suppresses B cell responses and osteoclastic bone erosion in rheumatoid arthritis. Acta Pharmacologica Sinica. 2021; 42: 1653–1664. https://doi.org/10.1038/s41401-020-00578-0.

[25] Shaul ME, Zlotnik A, Tidhar E, Schwartz A, Arpinati L, Kaisar-Iluz N, *et al*. Tumor-Associated Neutrophils Drive B-cell Recruitment and Their Differentiation to Plasma Cells. Cancer Immunology Research. 2021; 9: 811–824. https://doi.org/10.1158/2326-6066.CIR-20-0839.

[26] Udagawa N, Koide M, Nakamura M, Nakamichi Y, Yamashita T, Uehara S, *et al*. Osteoclast differentiation by RANKL and OPG signaling pathways. Journal of Bone and Mineral Metabolism. 2021; 39: 19–26. https://doi.org/10.1007/s00774-020-01162-6.

[27] De Leon-Oliva D, Barrena-Blázquez S, Jiménez-Álvarez L, Fraile-Martinez O, García-Montero C, López-González L, *et al*. The RANK-RANKL-OPG System: A Multifaceted Regulator of Homeostasis, Immunity, and Cancer. Medicina (Kaunas, Lithuania). 2023; 59: 1752. https://doi.org/10.3390/medicina59101752.

[28] Dybowski S, Torke S, Weber MS. Targeting B Cells and Microglia in Multiple Sclerosis With Bruton Tyrosine Kinase Inhibitors: A Review. JAMA Neurology. 2023; 80: 404–414. https://doi.org/10.1001/jamaneurol.2022.5332.

[29] Ringheim GE, Wampole M, Oberoi K. Bruton's Tyrosine Kinase (BTK) Inhibitors and Autoimmune Diseases: Making Sense of BTK Inhibitor Specificity Profiles and Recent Clinical Trial Successes and Failures. Frontiers in Immunology. 2021; 12: 662223. https://doi.org/10.3389/fimmu.2021.662223.

[30] Langrish CL, Bradshaw JM, Francesco MR, Owens TD, Xing Y, Shu J, *et al*. Preclinical Efficacy and Anti-Inflammatory Mechanisms of Action of the Bruton Tyrosine Kinase Inhibitor Rilzabrutinib for Immune-Mediated Disease. Journal of Immunology (Baltimore, Md.: 1950). 2021; 206: 1454–1468. https://doi.org/10.4049/jimmunol.2001130.